

# Volume-constrained Image Registration for Pre- and Post-operative CT Liver Data

Björn Beuthien <sup>a,b</sup>, Nils Papenberg <sup>c</sup>, Stefan Heldmann <sup>c</sup>, Bernd Fischer <sup>a</sup>

<sup>a</sup>Institute of Mathematics, University of Lübeck, Germany;

<sup>b</sup>Graduate School for Computing in Medicine and Life Sciences, University of Lübeck, Germany;

<sup>c</sup>Fraunhofer MeVis, Group Lübeck, Germany

## ABSTRACT

The resection of a tumor is one of the most common tasks in liver surgery. Here, it is of particular importance to resect the tumor and a safety margin on the one hand and on the other hand to preserve as much healthy liver tissue as possible. To this end, a preoperative CT scan is taken in order to come up with a sound resection strategy. It is the purpose of this paper to compare the preoperative planning with the actual resection result. Obviously the pre- and postoperative data is not straightforward comparable, a meaningful registration is required. In the literature one may find a rigid and a landmark-based approach for this task. Whereas the rigid registration does not compensate for nonlinear deformation the landmark approach may lead to an unwanted overregistration. Here we propose a fully automatic nonlinear registration with volume constraints which seems to overcome both aforementioned problems and does lead to satisfactory results in our test cases.

**Keywords:** Image Registration, Volume-Preservation, Constrained Optimization, Liver Surgery

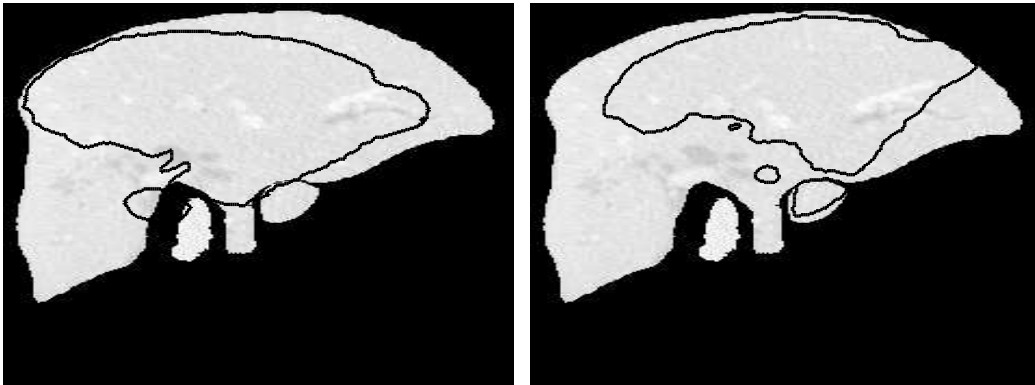
## 1. DESCRIPTION OF PURPOSE

For patients with liver tumors, surgical resection is the main curative treatment. The surgery is delicate. On the one hand the surgeon has to resect the tumor and a safety margin around it. On the other hand a certain amount of healthy liver volume needs to be preserved such that the patient can survive. Since the liver is pervaded with several vessels, the resection is even more difficult. Therefore a preoperative surgery planning is realized based on CT data.<sup>1</sup> Due to the fact that the liver is a homogeneous organ, for the surgeon it is difficult to see where the exact resection line is, he is guided by registered ultrasound images. Between the second and third day after the surgery another CT scan is taken. At this stage the swelling should nearly be disappeared and the regeneration of the lost tissue is hardly noticeable. For evaluation purpose of the surgery, it is necessary to know how the preoperative planning was turned over. This paper focuses on this part. Here we present a registration of the pre- and postoperative CT liver data. The purpose of the registration is to detect areas of the preoperative liver that are still present although they should not be and vice versa. Similar work was presented before by Dumpuri et al.<sup>2</sup> and Lange et al.<sup>3</sup> The first approach is based on a rigid registration. In this case the advantage is the volume preserving behaviour but the method is not capable to deal with the movement of the organ and the impact of the mobilization of the liver. The approach proposed by Lange et. al. is a landmark-based registration. Here, nonlinear deformations are possible but the registration is not volume preserving. Additionally the landmarks need to be set. In contrast to these two approaches we use an automatic nonparametric registration with volume constraints. The benefit of this approach is that we use much more information for the registration and are capable of dealing with nonlinear deformations while stopping the postoperative liver increasing its volume.

---

Further author information: (Send correspondence to B. Beuthien)

B. Beuthien: E-mail: beuthien@math.uni-luebeck.de, Telephone: 49 451 7030420



(a) preregistration on masked liver

(b) preregistration on masked venous system

Figure 1. Results of the rigid preregistration with different input data. 2D slides of the preoperative liver with contours of the deformed postoperative liver are shown. Here, we shown the resulting deformation fields applied both to the masked liver with the venous vessel system, although they come from different input data

## 2. METHODS

In this section we present the scheme for registering a postoperative liver volume  $\mathcal{T}(x)$  to a preoperative liver volume  $\mathcal{R}(x)$ ,  $x \in \Omega$ , with respect to volume preserving constraints. For this problem we can revert to the abdominal CTs of the pre- and postoperative liver. Furthermore, segmentations of the livers as well as segmentations of all vascular systems of the liver are assumed to be given. For our registration purposes, we use the segmentation of the liver as well as the one of the venous vessel system as masks for the given abdominal CTs. The usage of the venous vessel system will provide points of orientation, especially the region of the porta hepatis will turn out to be quite useful. Prior to the nonlinear registration we perform a preregistration. It is nothing but a rigid registration producing a rough alignment. In contrast to an affine linear or landmark registration, no change of volume can occur. Instead of performing the rigid registration on the complete liver we just use the venous vessel system. If we would use the full data here, the danger of trapping into a local minimum is considerably higher, as the comparison of the two techniques in Figure (1) indicates. As a starting point for the rigid registration we let the centroids of the two images overlap by a translation. The nonlinear alignment is done by an elastic registration. Since we are dealing with monomodal data we use the Sum-of-Squared-Differences as the distance measure, i.e.

$$\mathcal{D}(\mathcal{R}, \mathcal{T}, y) = \frac{1}{2} \int_{\Omega} (\mathcal{T}(y(x)) - \mathcal{R}(x))^2 dx, \quad (1)$$

where  $y$  is the deformation field. Assuming that the deformation of the liver is elastic, the choice of the smoother is the elastic one, i.e.

$$\mathcal{S}(y) = \frac{1}{2} \int_{\Omega} \sum_{j=1}^d \|\nabla y_j(x)\|^2 + \text{div}^2(y(x)) dx, \quad (2)$$

where  $\mu$  and  $\lambda$  are the so-called Lamé constants. To disable the volume change, enforced by the nonlinear registration, we include volume-preserving constraints similar to the work of Haber and Modersitzki,<sup>4</sup> i.e. we use voxel-wise volume constraints. Since it is possible that the liver is folding after the surgery, the constraints are just evaluated in the liver region  $\Omega_L = \{x | \text{mask of liver has a value greater than zero at } x\}$ . The registration is done in a discretize-then-optimize framework, i.e. we first discretize the functional and the constraints and then use numerical optimization methods to find a minimizer of the problem. For more information regarding this approach see e.g.<sup>5</sup> The minimization problem reads as follows. Find a deformation field  $y$  which minimizes the joint functional

$$\begin{aligned} \mathcal{J}(y) &= \mathcal{D}(\mathcal{R}, \mathcal{T}, y) + \alpha \mathcal{S}(y) \\ \text{s.t. } \det(\nabla y(x)) - 1 &= 0, \quad x \in \Omega_L. \end{aligned} \quad (3)$$

We choose the determinant of the Jacobian as description of the volume constraints, because here we have for  $n$  voxels  $n$  constraints instead of  $5n$  resp.  $6n$  constraints for volume constraints based on a decomposition

into tetrahedrons.<sup>4</sup> However, the price paid for this elegant approach is the fact that the discretization of  $\det(\nabla y)$  is a delicate task. In principle a lousy discretization may lead to unwanted foldings. However, this has not been observed in our test runs but nevertheless will be investigated in future work. For notational convenience, we will explain the discretization of the constraint in 2D, the extension to 3D is straight forward. Let  $x = (x_1, x_2)^T \in \Omega \subset \mathbb{R}^2$  and  $y(x) = (y_1(x), y_2(x))^T$ . Consider a cell-centered grid discretization in Figure 2. Choosing this discretization seems to be a good choice since we can easily assign a coordinate to each voxel.

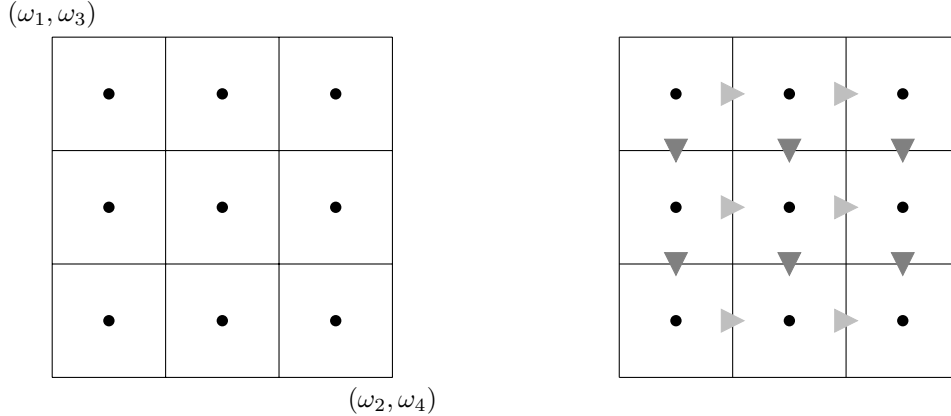


Figure 2. On the left we can see a cell-centered grid discretization. On the right a simple discretization of the partial derivatives can be seen. The positions of the derivatives in  $x_1$ -direction are marked with a triangle pointing downward, the positions of the derivatives in  $x_2$ -direction with a triangle in lightgray pointing right

However, we will see that a simple discretization has several disadvantages. The discretization of our constraints

$$\det(\nabla y(x)) = \det \left( \nabla \begin{pmatrix} y_1(x) \\ y_2(x) \end{pmatrix} \right) = \det \begin{pmatrix} \frac{\partial y_1(x)}{\partial x_1} & \frac{\partial y_1(x)}{\partial x_2} \\ \frac{\partial y_2(x)}{\partial x_1} & \frac{\partial y_2(x)}{\partial x_2} \end{pmatrix}, \quad (4)$$

involves in particular the one for partial derivatives. Using a cell-centered grid and a forward differences approximation, the derivatives are located on a staggered grid (see Figure 2). As we do not want to change the volume of the voxels, this simple discretization is not desirable for two reasons. Firstly, the derivatives in  $x_1$ - and  $x_2$ -direction are not computed at the same coordinates. The other reason stems from the fact, that both of them are not located at the center of the voxel whose volume we want to preserve. With the following discretization we satisfy both aspects.

In order to establish a good discretization we use a nodal grid for the constraints as it can be seen in Figure 3. Here, it is possible to compute a good approximation of partial derivatives at the cell-centers in both directions. Therefore let  $\Omega = (\omega_1, \omega_2) \times (\omega_3, \omega_4)$  and  $m = (m_1, m_2)$  the number of voxels. Then, with the voxel-spacing  $h = (h_1, h_2) = (\frac{\omega_2 - \omega_1}{m_1}, \frac{\omega_4 - \omega_3}{m_2})$ , the coordinates of the nodal grid are given by  $x_{i,j} = (\omega_1 + ih, \omega_3 + jh)$  for  $i = 0, \dots, m_1$  and  $j = 0, \dots, m_2$ . Consider a single cell as shown in Figure 3 spanned by the coordinates  $x_{i,j}, x_{i+1,j}, x_{i,j+1}$  and  $x_{i+1,j+1}$ . We compute exemplarily the partial derivative of  $y_1$  in  $x_1$ -direction at cell-centered positions by

$$\frac{\partial y_1(x_{i,j}^c)}{\partial x_1} \approx \frac{b - a}{h_1} \quad (5)$$

where

$$\begin{aligned} a &\approx \frac{1}{2} (y_1(x_{i,j}) + y_1(x_{i,j+1})) \\ b &\approx \frac{1}{2} (y_1(x_{i+1,j}) + y_1(x_{i+1,j+1})). \end{aligned} \quad (6)$$

The other partial derivatives are computed analogously. Now we satisfy both properties. Figures 4 to 6 illustrate the constraints for a rigid and a nonlinear registration in 2D.

The applied minimization algorithm is a generalized Gauss-Newton method as used by Olesch et.al.<sup>6</sup>

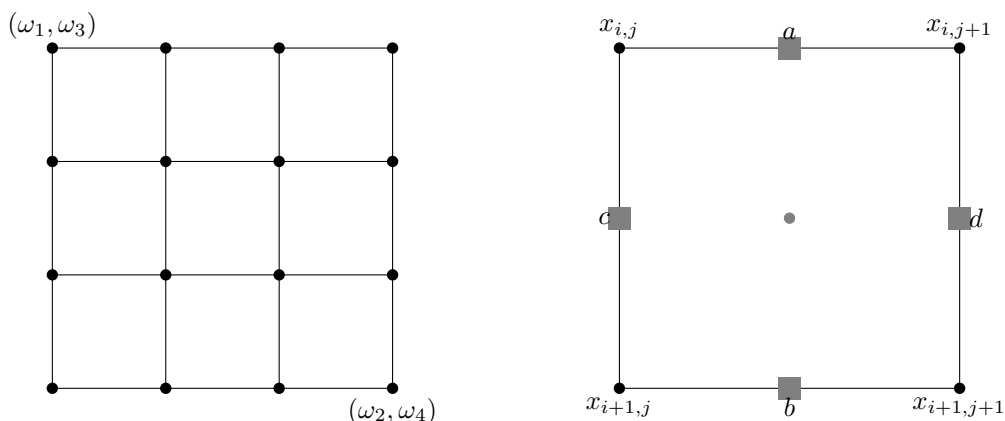
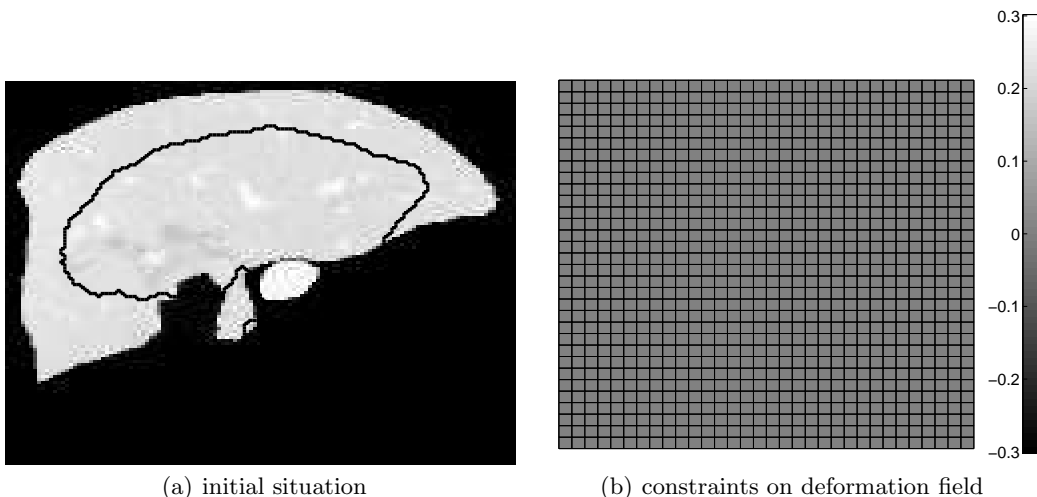


Figure 3. On the left we can see a 2D nodal grid for an area with 3 cells in both directions. On the other side one cell is picked out. Here the interesting points for the computation of the partial derivatives are shown



(a) initial situation

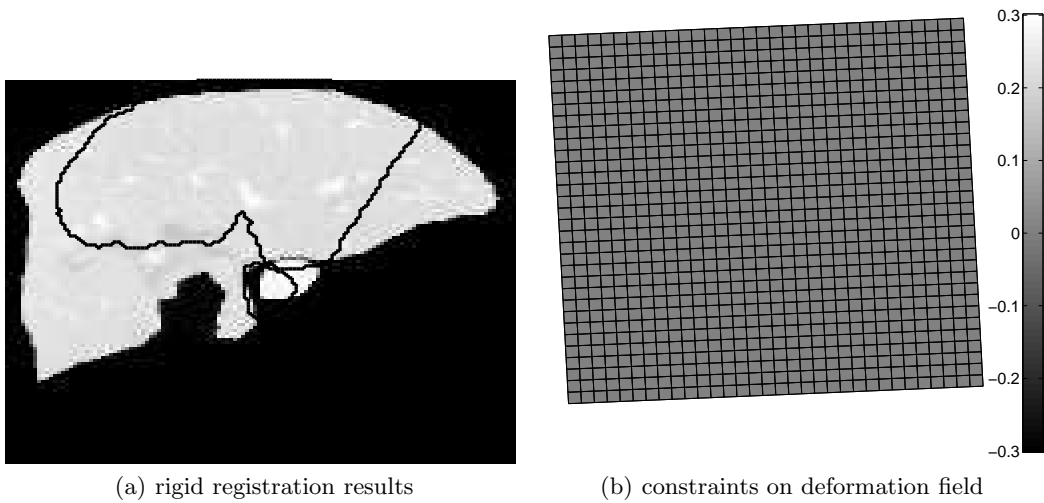
(b) constraints on deformation field

Figure 4. Here we can see the situation at the beginning of the registration (before rigid). On the left side the reference with the boundary of the template can be seen. On the right side the deformation field, in this case the identity, with the discretized constraints  $\det(\nabla y) - 1$  are shown. As expected the constraints are zero everywhere

### 3. RESULTS

In this section we will demonstrate the capability of the described method. For this purpose, we use abdominal pre- and postoperative CT scans with a contrast agent used to enhance the vascular system. The preoperative CT is of the size  $512 \times 512 \times 206$  with a resolution  $0.7441 \times 0.7441 \times 1.0000$  mm. The size of the post operative CT is  $512 \times 512 \times 221$  with a resolution of  $0.6836 \times 0.6836 \times 1.0000$  mm. Since we are interested in the registration of the livers we choose a ROI of size  $297 \times 236 \times 188$  and  $272 \times 270 \times 213$  for the preoperative resp. postoperative image. For the registration we use the masked area of the liver plus the venous vessel system. The starting data can be seen in Figure (7). The rigid preregistration is based solely on the venous vessel system which was on top scaled down to  $16^3$  voxels. Through the rigid registration the value of the distance measure could be reduced to 45% with respect to the starting data. The nonlinear registration is done with a multi-level approach with an image size  $32^3$  at the end and regularization parameter  $\alpha = 3 \cdot 10^6$ . Figure (8) shows the final results which appear to be quiet satisfactory. Here we can see clearly that the both images are still well aligned at the porta hepatis. This region is of particular interest since we know there should be still an overlap. In contrast to the preregistration the other parts of the liver are aligned much better as well and the distance measure is reduced by about another 45% concerning the value of the rigid registration.

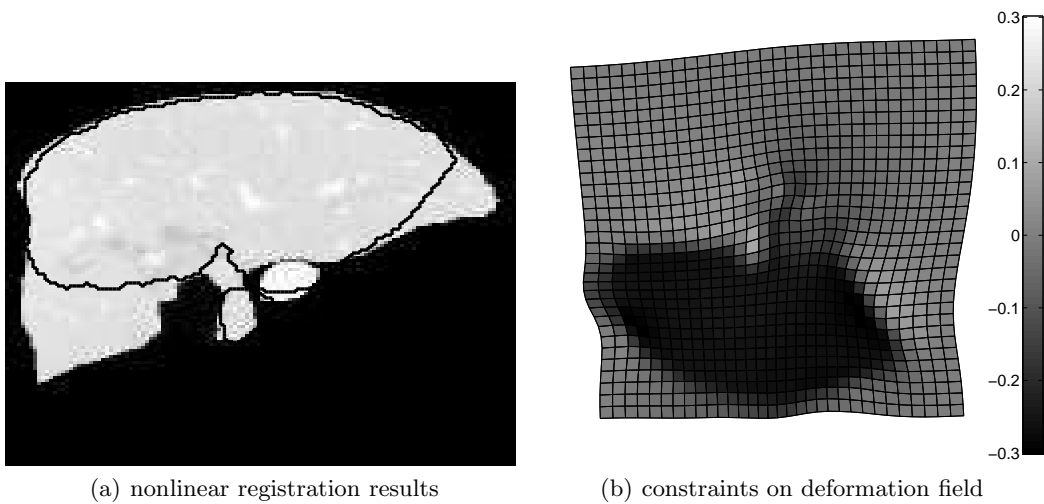
For the second test case we consider a preoperative CT of size  $512 \times 512 \times 266$  with a resolution of  $0.715 \times$



(a) rigid registration results

(b) constraints on deformation field

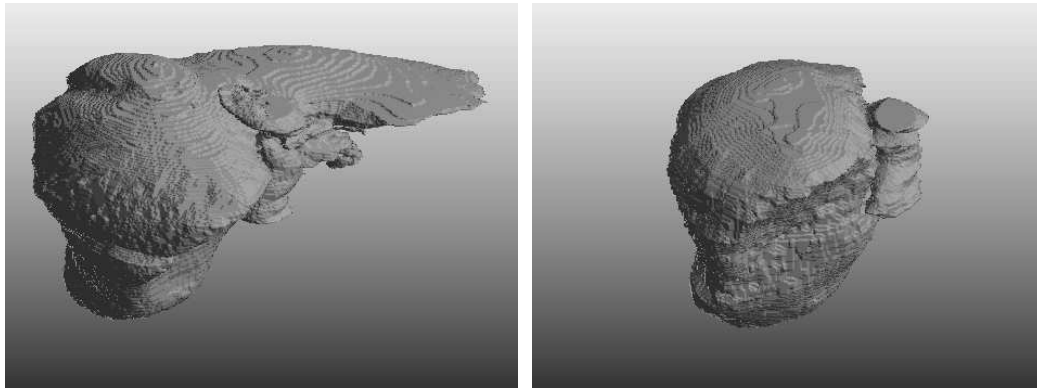
Figure 5. We can see the results after a simple rigid registration. Again on the left side the reference with the boundary of the deformed template are shown. The right side shows the corresponding deformation field with the discretized constraints  $\det(\nabla y) - 1$ . Since a rigid deformation is volume preserving the constraints are zero everywhere



(a) nonlinear registration results

(b) constraints on deformation field

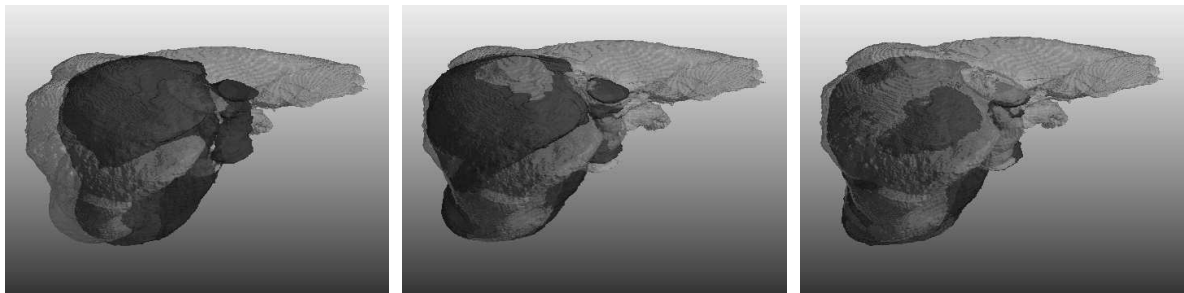
Figure 6. The figure illustrates the results of an exemplarily nonlinear registration without applying the constraints for volume preservation. To the left we see the reference with the contours of the deformed template. On the other side deformation field is shown extended by the discretized constraints  $\det(\nabla y) - 1$  computed afterwards. We notice in both images a strong volume change



(a) preoperative liver (reference)

(b) postoperative liver (template)

Figure 7. Masked pre- and postoperative liver with venous vessel system from the CT scans of the first test run



(a) initial situation

(b) result after preregistration

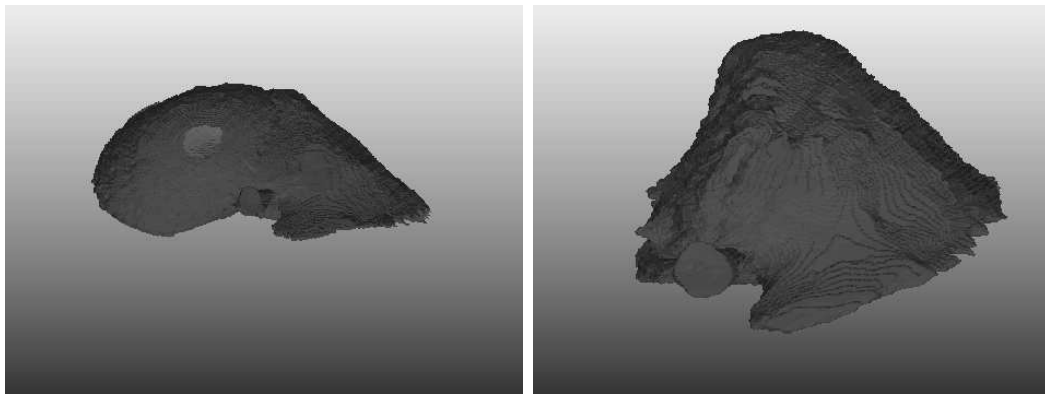
(c) final result

Figure 8. Results of the automatic registration of a postoperative to a preoperative liver. The light preoperative transparent 3D surface with the darker red transparent surface of the deformed postoperative liver can be seen after the preregistration and the following nonlinear registration

$0.715 \times 1$  mm and a postoperative CT of size  $512 \times 512 \times 301$  with a resolution of  $0.684 \times 0.684 \times 1$  mm. The ROIs are of size  $398 \times 333 \times 266$  for the preoperative and  $361 \times 299 \times 210$  postoperative scan. The initial situation is shown in Figure 9. As in the previous test case, we start with a multi-resolution rigid registration on the venous vessel system. Through this, the distance measure could be reduced by about 10%. As expected some misaligned parts can still be seen. However, the region of the porta hepatis could be aligned well, so we get a good initial situation for the nonlinear registration. The image in the middle of Figure 10 illustrates this result. For the nonlinear registration we emphasize the region of the IVC and use the masked liver with the venous vessel system again. The multi-resolution approach ends at a size of  $32^3$  and we choose the regularization parameter  $\alpha = 2 \cdot 10^6$ . Through the nonlinear registration the distance measure is brought down to 60% with respect to the result of the rigid registration. As it can be seen in Figure 10 the postoperative liver fits the preoperative one very good. Actually the part of the porta hepatis is aligned even better.

#### 4. NEW OR BREAKTHROUGH OF THE WORK

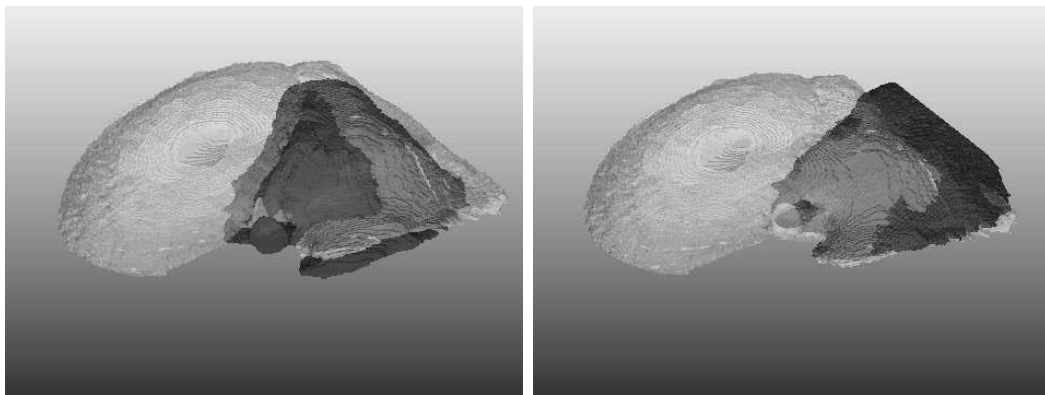
The validation of image-guided liver-surgery results is a problematic task. Since we do not compare the same objects, a perfect fit is not the aim of the registration anymore. In this paper we introduce for the first time a fully automatic approach for the nonlinear registration of a postoperative to a preoperative liver. For this purpose we start with a rigid preregistration based on the vascular system followed by a nonlinear registration with volume-preserving constraints in the liver region. Thus we disable the enforced volume change of the postoperative liver and are still capable to take care of nonlinear deformations. As we could see this method leads to promising results. Currently we are working on a validation of the proposed method for a collection of post/pre-operative livers. Therefore we plan to use landmarks set by a clinical expert to validate the registration result and as a basis for discussions with the expert.



(a) preoperative liver (reference)

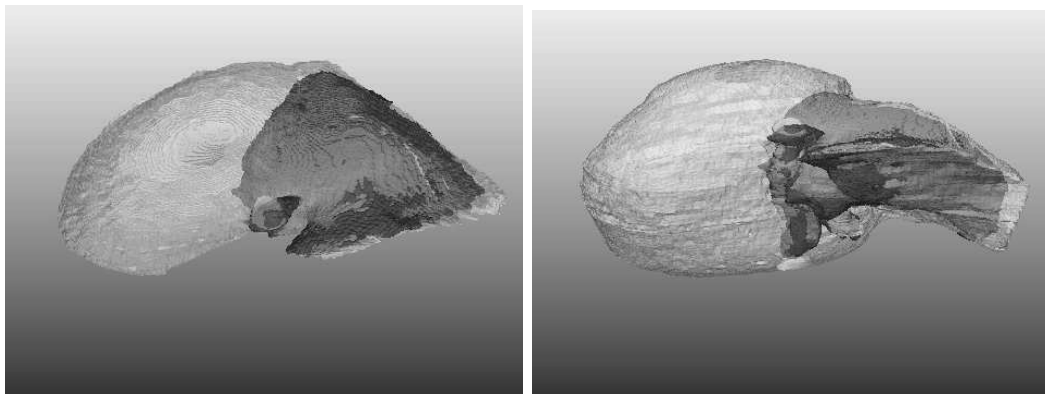
(b) postoperative liver (template)

Figure 9. Masked pre- and postoperative liver with venous vessel system from the CT scans of the second test run



(a) initial situation

(b) result after preregistration



(c) final result - perspective 1

(d) final result - perspective 2

Figure 10. Results of the automatic registration of a postoperative to a preoperative liver for the second case. The light preoperative transparent 3D surface with the darker red transparent surface of the deformed postoperative liver can be seen after the preregistration and the following nonlinear registration

## ACKNOWLEDGMENTS

We thank Christoph Logge for providing the CT-data which were processed by the MeVisLiverAnalyzer and Janine Olesch and Matthias Conrad for providing the Matlab implementation of the generalized Gauss-Newton method.

## REFERENCES

- [1] Lang, H., Radtke, A., Hindennach, M., Schroeder, T., Frühauf, N. R., Malagó, M., Bourquain, H., Peitgen, H. O., Oldhafer, K. J., and Broelsch, C. E., “Impact of virtual tumor resection and computer-assisted risk analysis on operation planning and intraoperative strategy in major hepatic resection.,” *Archives of surgery (Chicago, Ill. : 1960)* **140** (July 2005).
- [2] Dumpuri, P., Clements, L., Li, R., and Waite, J., “Comparison of pre/post-operative CT image volumes to preoperative digitization of partial hepatectomies: a feasibility study in surgical validation,” *Proceedings of SPIE* (Jan 2009).
- [3] Lange, T., Wörz, S., Rohr, K., and Schlag, P. M., “Landmark-based 3D elastic registration of pre-and postoperative liver CT data,” *Bildverarbeitung Für Die Medizin 2009: Algorithmen-Systeme-Anwendungen* (Jan 2009).
- [4] Haber, E. and Modersitzki, J., “Image registration with guaranteed displacement regularity,” *International Journal of Computer Vision* (Jan 2007).
- [5] Modersitzki, J., [*FAIR: Flexible Algorithms for Image Registration*], SIAM, Philadelphia (2009).
- [6] Olesch, J., Papenberg, N., Lange, T., and Conrad, M., “Matching CT and ultrasound data of the liver by landmark constrained image registration,” *Proceedings of SPIE* (Jan 2009).